Journal of Mining and Environment (JME), Vol. 12, No. 1, 2021, 219-233

Shahrood University of Technology

Iranian Society of Mining Engineering (IRSME)

Journal of Mining and Environment (JME)

journal homepage: www.jme.shahroodut.ac.ir

THOMSON REUTERS

Studying Effect of Modifying Nano-Mineral Adsorbents on Efficiency of Dye Removal from Industrial Effluents

Azadeh Agah[1*] and Nasrin Falahati[2]

1. Mining department, engineering Faculty, University of Sistan and Baluchestan, Zahedan, Iran
2. Mining Engineering Department, Arak University of Technology, Arak, Iran

Article Info

Received 30 September 2020

Received in Revised form 04 December 2020

Accepted 7 December 2020

Published online 7 December 2020

DOI:10.22044/jme.2020.10122.1950

Keywords

Adsorption
Tonsil
Nano-clay
Dye removal
Industrial effluents

Abstract

In this research work, the potential capability of nano-clay and tonsil, as low-cost and domestic adsorbents, for the elimination of a cationic dye, (CR18) from contaminated water is investigated. The surface properties of the adsorbents are studied by means of the scanning electron microscopy (SEM) and X-ray diffraction techniques. The effects of the initial dye concentration, pH, stirring speed, contact time, and adsorbent dosage are investigated at 25. The results obtained show that the dye adsorption data from the nano-clay and tonsil experiments fit well to the Langmuir and Freundlich isotherms, respectively. The results of dye adsorption kinetics demonstrate that the adsorption system follows a pseudo-second-order model with a satisfactory correlation value (R=99%).The adsorption thermodynamics is also studied, concluding that the adsorption process is spontaneous and physically controlled. Under the optimum conditions (pH of 7, stirring speed of 200 rpm, CR18 concentration of 30 ppm and contact time of 30 min), the adsorption capacities of the mixed adsorbents show the maximum adsorption efficiency at the tonsil:nano-clay weight ratio of 1:2.

1. Introduction

Many industrial units use dyes, especially synthetic dyes, for coloring their products, consuming a considerable amount of water. These include the dyestuff, textile, paper, and plastic industries. Such industries generate, quite naturally, a considerable amount of colored wastewater as well [1-3].

Dyes are very difficult to decompose biologically, are toxic to the aquatic life, and pose serious problems for the local living organisms due to their carcinogenicity and toxicity features [4, 5 and, 6]. Also their solutions are among the major environmental problems; they contain a large amount of suspended solids with high COD (chemical oxygen demand) concentrations and highly fluctuating pH values [7-10]. This is why it is very difficult to treat such streams by the formal physico-chemical and biological treatment procedures. Hence, the search for novel, economical, and suitable materials for the removal of dyes is of paramount importance. Cationic dyes are water-soluble dyes that yield colored cations in aqueous solutions. Their major chemical groups are diazahemicyanines, triarylmethanes, cyanines, hemicyanines, thiazines, oxazines, and acridines [11, 12].

Adsorption methods have been preferred to some other methods of removing colored waste effluents produced by industrial sites including the membrane separation process, chemical oxidation, coagulation, electrochemical precipitation, and ion exchange. This is due to their cheapness and the high quality of the treated effluents, particularly for well-designed adsorption processes [13-17]. Adsorption is a surface phenomenon, and refers to the accumulation of substances near the interface

Corresponding author: azadeh.agah@yahoo.com (A. Agah.).

with a mainly chemical engineering approach. In this regard, surface forces, concentration of the materials on the adsorbent surface, and porosity are considered to be the controlling factors [18-23]. An adsorption process is favorable when the local concentration becomes greater than the bulk solution concentration [24]. In order to define the equilibrium relation between the quantities of the adsorbed material and the concentration in the bulk fluid phase under a constant temperature, the adsorption isotherms have always been fundamental tools [25, 26].

Activated carbon is the most broadly used adsorbent for the removal of dyes due to its high ability for the adsorption of organic substance; it is, however, too expensive to be widely used in wastewater treatment industries [27 and 28]. Some of the reported adsorbents contain clay minerals (kaolinite, bentonite) [29-37], zeolites [38-40], siliceous materials (alunite, perlite, silica beads) [41-47], agricultural wastes (bagasse pith, maize cob, rice husk, coconut shell, banana and orange peel, etc.) [10, 15, 48-57], industrial waste products (metal hydroxide sludge, waste carbon slurries, steel plant slag) [1, 14, 52, 58-60], bio sorbents [28, 61-68], and others (starch, cyclodextrins, cotton) [1, 67-72].

Application of clay minerals as adsorbents to remove pollutants has lately been paid a growing attention because they are readily accessible, inexpensive, and environmental friendly. The final goal is that, in the future, clay adsorbents be used in order to establish a cost-effective adsorption system, particularly for dye removal. The uptake process is usually affected by some environmental factors such as the pH, contact time, initial dye concentration, stirring speed, ionic strength, adsorbent dosage, temperature, and type of dye.

Due to the quick accessiblity and low cost of the clay mineral in Iran, the present work was under taken with the following special objectives: 1. to study the performance and efficiency of nano- clay in the removal of dyes by adsorption from industrial effluents; 2. to define the effects of the pH, initial dye concentration, contact time, and stirring speed on the adsorption ability of nano-clay as an adsorbent; 3. to check the applicability of the Temkin, Langmuir, and Freundlich isotherms, pseudo-first-order adsorption and pseudo-second-order adsorption kinetics; 4. to prepare additional information on the adsorption of the dye by nano-clay; and5. to recognize the adsorption mechanism of the dyes by the nano-clay based on the factors such as the adsorbent ability, free energy variation, and entropy and enthalpy change.

2. Materials and Methods

The source material for tonsil is silicon dioxide, which is a chemical composite made of an oxide of silicon with the chemical formula SiO_2 . The laboratory instruments used to measure the changes in each variable during the experiment were a heater (model: VS-130SH) for temperature measurement, a digital weighing machine (model: Sartorius) for mass measurement, a UV-visible spectrophotometer (model: Perkin-Elmer lambda 25) for determining the dye uptake, a pH-meter (model: Mettler Toledo), a centrifuge machine (model: Hettich EBA 20) for separation of the adsorbent particles from the effluents after dye adsorption tests, and a Jar-test equipment (model: Velp EQ-ER-13) for stirring the adsorbent particles in the solution. Moreover, SEM (model: LEO 1455VP) and XRD (model: Advanced D8) were used in order to study the morphology, the structure of tonsil, and mineral characterization of the sample. The pH values of the solutions were regulated by 2 M NaOH and H_2SO_4 solutions. The dye was provided from Alvansabet Ltd. (Iran), and the other chemicals used were obtained from the Merck Company. Table 1 shows the chemical characterization of cationic red 18, used as a model pollutant. Figure 1 shows the chemical structure of cationic red 18 (CR18).

Table 1: Cationic red 18 properties at a constant concentration of 30 ppm in the solution.

Name	Molecular formula	Molecular weight (g/mol)	λ_{max} (nm)	Extinction coefficient (L.cm.Mol^{-1})
Cationic red 18	$C_{19}H_{25}C_{12}N_5O_2$	426.3	487.5	6435

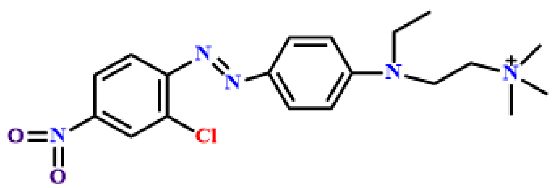

Figure 1. Chemical structure of CR18.

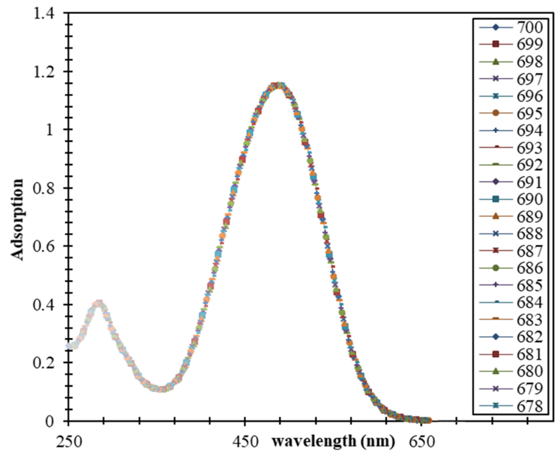

Figure 2. The spectrophotometry plot observed for CR18.

As it can be seen in Figure 2, the maximum absorbance occurs in a wavelength of about 487 nm. This wave-length could be used in to determine the dye concentration and the initial absorbance of the other parameters.

2.1. Adsorption studies

The sorption measurements were performed by mixing several values of tonsil (0.0075-0.03 g) for CR18 in jars including 250 mL of a dye solution (30 mg/L) at different pH values (2–12). The pH values were investigated in order to find the optimal pH-level at which the maximum dye removal is was attained. The experiments were performed at concentrations of 20, 30, 40, 50, and 60 mg/L, by applying 0.03 g tonsil for CR18 at pH 12. The adsorption changes were measured at certain time intervals, including 5, 10, 15, 30, 45, 60, and 120 min. Various stirring rates were used, and there were important discrepancies among the stirring rates of 45 up to 200 rpm. Finally, the samples obtained were centrifuged by Hettich EBA20, and next, the dye concentration was defined. The adsorption efficiency of CR18 on tonsil was estimated by defining the decrease percentage of the absorbance at 485.5 nm by Equation (1) [73].

$$\text{Dye removal } (\%) = \frac{A_0 - A}{A_0} * 100 \quad (1)$$

Here, A_0 denotes the original absorbance, and A is the last absorbance of the dye solution. Freundlich and Langmuir isotherm equations were checked in the current research.

The Langmuir equation can be given as:

$$q_e = \frac{Q_0 K_L C_e}{1 + K_L C_e} \quad (2)$$

Where q_e is the quantity of the dye adsorbed on tonsil at the equilibrium, Q_0 is the maximum adsorption capacity, K_L is the equilibrium constant, and C_e is the equilibrium concentration of the dye solution.

The Freundlich isotherm is originated by presuming a non-uniform distribution of the adsorption heat over the heterogeneous surface. It can be written as follows [74, 75].

$$q_e = K_F C_e^{1/n} \quad (3)$$

Here, K_F denotes the adsorption capacity at unit concentration and 1/n is the adsorption intensity. The Tamkin isotherm assumes that the adsorption heat of all molecules decreases linearly with increasing adsorption surface coverage, and the adsorption is described by a uniform distribution of the binding energy, up to the maximum binding energy. The Temkin equation can be defined by:

$$q_e = \frac{RT}{b} \ln(A_T) + \frac{RT}{b} \ln(C_e) \quad (4)$$

Where $A_T\ (L/g)$ and $B = \frac{RT}{b}$ are the Temkin constants, T is the temperature (K), R is the universal gas constant of 8.314 $(J/mol.K)$, and b is related to the adsorption heat [76, 77].

2.2. Studies on characterization of tonsil and nano-clay

The results of SEM images obtained from the tonsil and nano-clay surfaces are shown in Figure 1. As it can be seen in the figure, the tonsil particles are relatively finer and more porous than the nano-clay particles in the same scale, indicating that the surface area of tonsil is larger than that of nano-clay. It also reveals the fact that the tonsil particles are mostly constitute the angular and sharp-corner forms, while the nano-clay samples show relatively circular particles on the surface. These differences could generate variations in the distribution form of charges on the surface of adsorbents and their stability in the solution media.

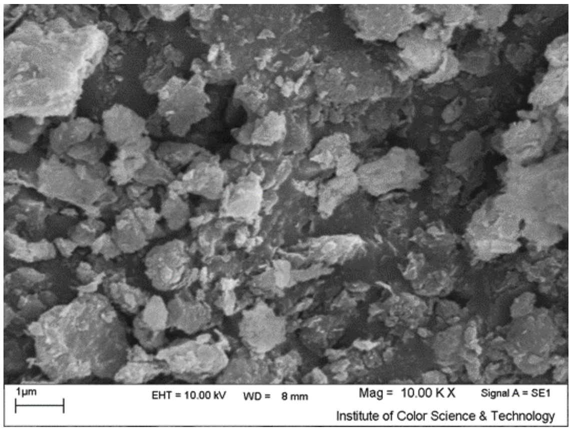

Figure 1a. SEM image of surface of the tonsil adsorbent (Scale: 1 micron).

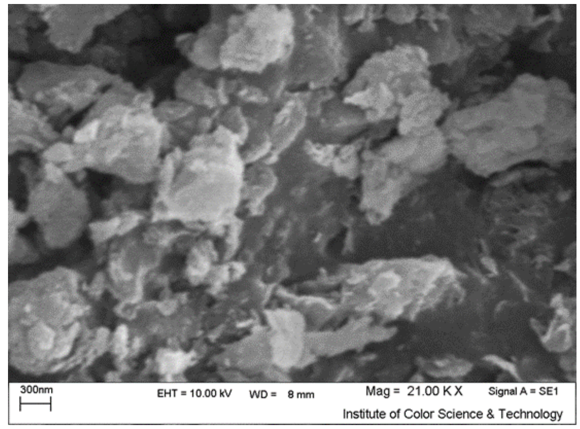

Figure 1b. SEM image of surface of the tonsil adsorbent (Scale: 300 nm).

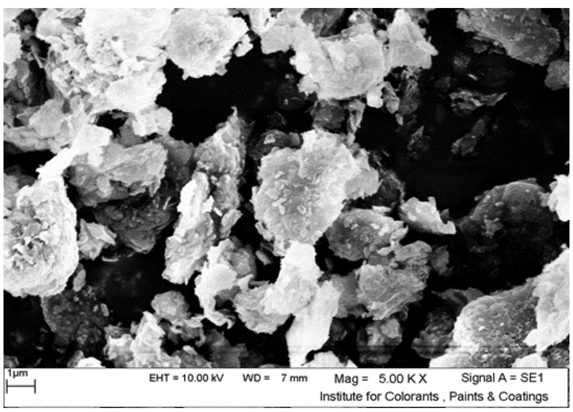

Figure 1c. SEM image of surface of the nano-clay adsorbent (Scale: 1 micron).

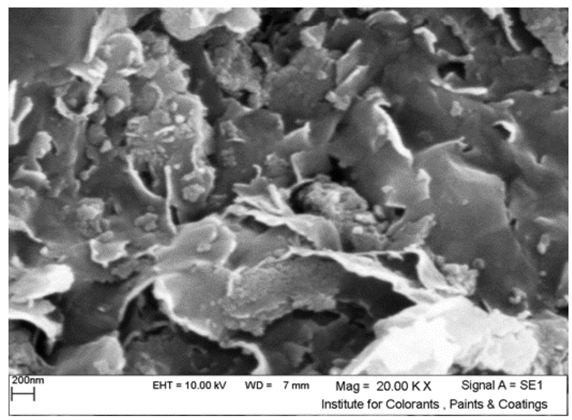

Figure 1d. SEM image of surface of the nano-clay adsorbent (Scale: 200 nm).

In order to identify and quantify the mineralogy of the crystalline compounds in the adsorbents, the X-ray diffraction (XRD) method was implemented. Figure 2 indicates that the major peak ($2\theta: 26.61$) refers to silicon dioxide, and also Tosudite is in the range of about $2\theta: 20.73^o$. Figure 3 shows that the main phase in the nano-clay sample, which is in the range of about $2\theta: 23^o$, refers to montmorillonite. Table 1 describes the abbreviations used in the XRD graphs in Figures 2 and 3.

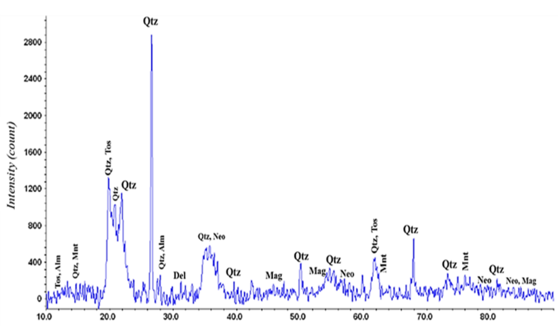

Figure 2. XRD graph of tonsil nano-particles.

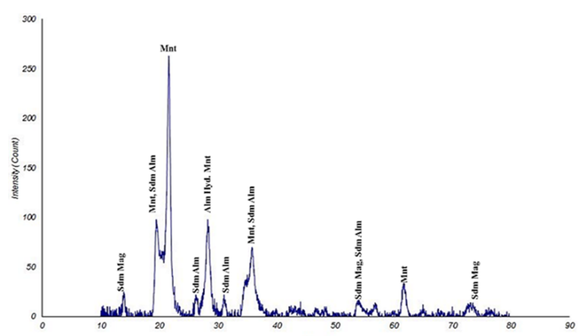

Figure 3. XRD graph for nano-clay.

Table 1. Identified phases and their abbreviations used in Figures 2 and 3.

No.	Mineral name	Abbreviation	Chemical formula
1	Delafossite	Del	$CuFeO_2$
2	Tosudite, Potassium Aluminum Silicate Hydroxide Hydrate	Tos	$(K,Ca)\ 0.8Al_6\ (Si,Al)\ 8O_{20}\ (OH)\ 10.4H_2O$
3	Aluminum Phosphate Silicate Tetrapropylammonium Hydroxide Hydrate	Alm	Al_2O_3-SiO_2-P_2O_5-$C_{12}H_{29}NO$- H_2O
4	Quartz	Qtz	SiO_2
5	Neodymium Zinc	Neo	NdZn
6	Manganese Sulfide	Mag	MnS
7	Montmorillonite	Mnt	$(Na,Ca)\ 0.3(Al,Mg)\ 2Si_4O_{10}\ (OH)_2\cdot xH_2O$
8	Aluminum Hydroxide Silicate	Alm Hyd	$(Al(OH)_2)\ 0.33Al_2\ Si_{3.67}Al_{0.33}O_{10})(OH)_2$
9	Sodium Aluminum Silicate Hydroxide Hydrate	Sdm Alm	$(Na,Ca)\ 0.3(Al,Mg)\ 2Si_4O_{16}\ (OH)_2\cdot xH_2O$
10	Sodium Magnesium Aluminum Silicate Hydroxide Hydrate	Sdm Mag	$Nax\ (Al,Mg)\ 2Si_4O_{10}\ (OH)_2\cdot xH_2O$

3. Results and Discussion

3.1. Effect of adsorbent concentration

In order to find the optimal concentration for each adsorbent, different values of tonsil and nano-clay were used. The optimum adsorbent concentration was estimated based on the dye removal content.

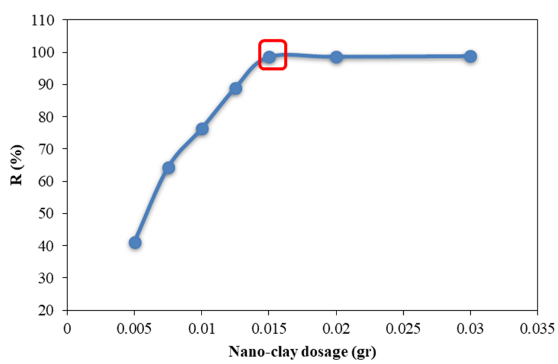

Figure 4. Adsorption efficiency of nano-clay at different concentrations, [dye] = 30 ppm.

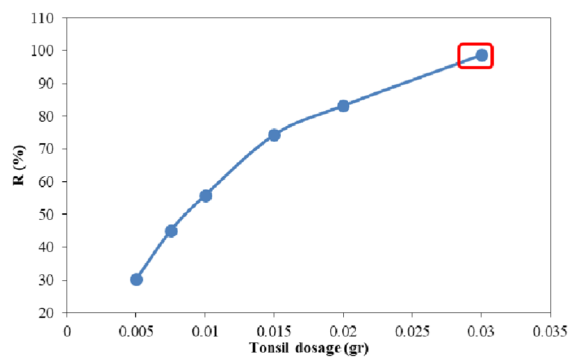

Figure 5. Adsorption efficiency of tonsil at different concentrations, [dye] = 30 ppm.

Figure 4 demonstrates that increasing the amount of nano-clay from 0.005 g up to 0.015g significantly improves the dye removal efficiency. However, a further increase in the amount of nano-clay (> 0.015 g) does not affect the dye removal efficiency, and shows a constant value. Considering the results of in Figure 5, increasing the amount of tonsil from 0.005 g to 0.03 g considerably increases the dye removal efficiency up to 68.45%. As highlighted in Section 2.2, the SEM images of nano-clay display a low surface area; thus it shows a limited adsorption capacity. Tonsil, on the other hand, could remove more dye from the solution media, due to its high surface area.

3.2. Effect of pH

The pH value is extremely important in removing dyes from a soluble medium, which affects the properties of the adsorbents and adsorbed substances. The first observation is that CR18 maintains its stability at the pH range of 2-12. The effect of pH on the yield of dye removal was investigated, and the results obtained were given in Figure 6.

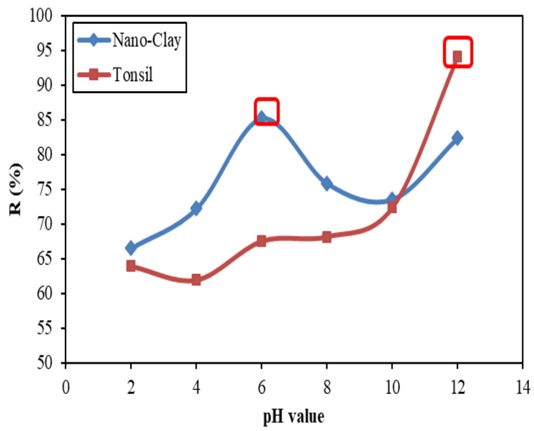

Figure 6. Effect of pH on CR18 adsorption onto tonsil and nano-clay.

Figure 6 reveals the fact that Nano-clay adsorbs dye particles in neutral media, while tonsil works better in alkaline solutions. Tonsil constitutes of numerous functional groups that are touched by the pH of solutions. Its nanoparticles are negatively charged at alkaline solutions, and because of having -N,N,N-Trimethyl-Ethanaminium in the structure of CR18, electrostatic attraction is dominant. At pH 12, a strong the electrostatic attraction is present between the surfaces of tonsil with negative electric charge, due to the ionization of the functional groups and positively charged cationic red 18 molecules [78,79]. However, the low adsorption of CR18 at an acidic pH is due to the existence of excessive amounts of H^+ ions, destabilizing cationic dyes, and competing with CR18 for available adsorption sites. Regarding this fact, the nano-clay and tonsil adsorption investigations were done in their optimum pH values including 6 and 12, respectively.

3.3. Effect of contact time

As adsorption proceeds, the adsorbed particles such as dyes cover the surface of the adsorbent, what, in turn, makes the adsorption process more difficult. Therefore, the contact time plays a key role in defining the adsorption capability. In order to find out the effect of the contact time on the dye adsorption, various time intervals including 5, 10, 15, 20, 30, 45, 60, 90 and 120 min, were considered together with different amounts of the adsorbents. The results obtanied are illustrated in the following figures.

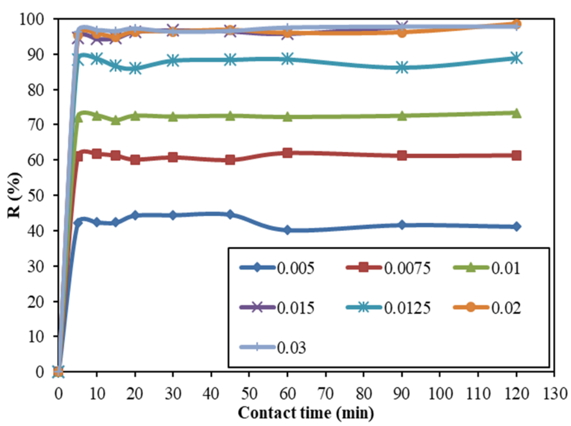

Figure 7. Effect of contact time on the adsorption efficiency of nano-clay, [dye] = 30 ppm.

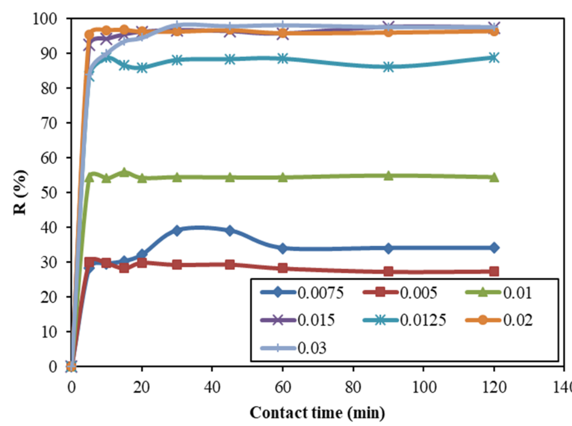

Figure 8. Effect of contact time on the adsorption efficiency of tonsil (0.005 and 0.0075), [dye] = 30 ppm.

Figures 7 and 8 indicate that increasing the amounts of nano-clay and tonsil from 0.005 g to 0.03 g enhances their adsorption efficiencies. Also the adsorption capacities of nano-clay and tonsil are almost complete at 5 min and 30 min after the beginning of the adsorption process, respectively. This shows that the process of reaching the maximum adsorption of tonsil, which is obtained at high amounts (98.34% at 0.03 g of tonsil after 30 min of the beginning of the adsorption process) is relatively slower than that of the nano-clay adsorbent.

3.4. Effect of dye concentration

The effect of various concentrations of CR18 including 20, 30, 40, 50, and 60 ppm was investigated with the adsorption times. The results obtained are given in Figures 9 and 10.

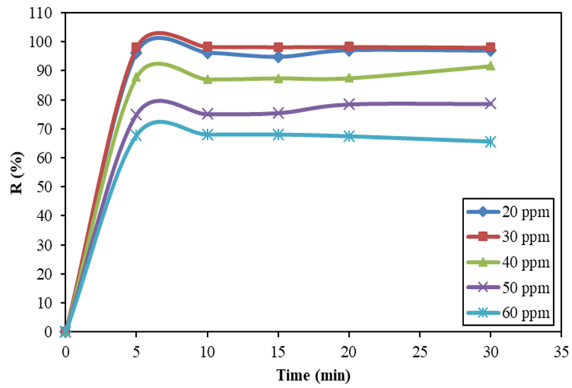

Figure 9. Effect of CR18 concentration on the adsorption efficiency of tonsil.

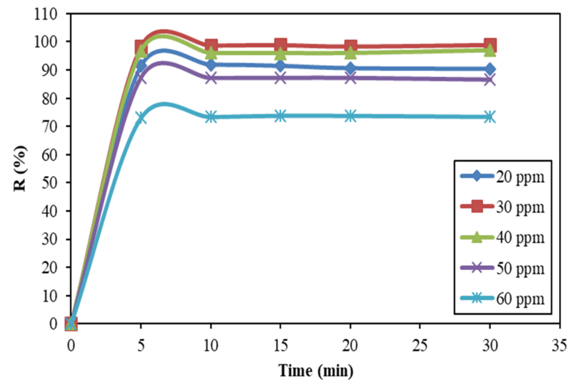

Figure 10. Effect of CR18 concentration on the adsorption efficiency of nano-clay.

It follows from Figures 9 and 10 that increasing the CR18 concentration from 20 ppm up to 30 ppm tends to enhance the adsorption efficiencies of tonsil and nano-clay. However, when the CR18 concentration exceeds 30 ppm, these adsorption efficiencies decrease. This is because by increasing the CR18 concentration, repellent forces between the CR18 molecules on the surfaces of the tonsil and nano-clay particles also increase, preventing more the CR18 molecules from being adsorbed. Therefore, the optimum CR18 concentration was considered 30 ppm for the rest of the experiments.

3.5. Effect of stirring speed

Adsorption kinetic is strongly controlled by the pore or film diffusion, and relies on the time and stirring speed in the system. Figure 11 reveals the fact that increasing the stirring speed tends to improve the adsorption efficiency of the adsorbents. However, the maximum adsorption was achieved at a stirring speed of 200 rpm, and a further increase in the stirring speed decreased the adsorption efficiencies of tonsil and nano-clay. In fact, since the adsorbents move very slowly at low stirring speeds, the surface layer of the liquid around the particle becomes very thick, which, in turn, prevents a further dye adsorption. However, at very high stirring speeds, where pore diffusion controls the adsorption rate, collision between the adsorbent molecules and the walls of the container leads to desorption. Having this fact in mind, the optimum stirring speed was considered 200 rpm for the rest of the experiments.

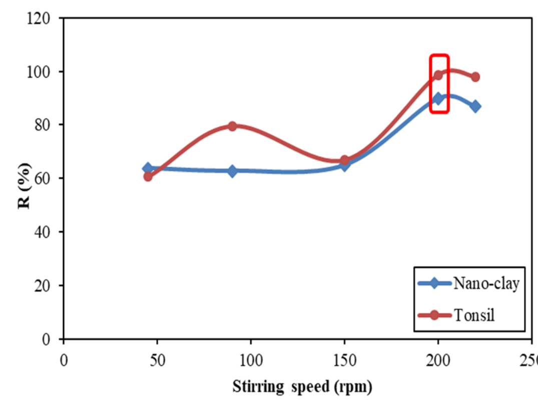

Figure 11. Effect of stirring speed on the adsorption efficiency.

3.6. Studies on adsorption isotherms

The equilibrium concentration of a substance dissolved on the surface of an adsorbent is related to the concentration of the solutes in solution by a curve called the adsorption isotherm. the Langmuir and Freundlich isotherms are the most commonly used isotherms; however, we also used the Temkin isotherm in this work.

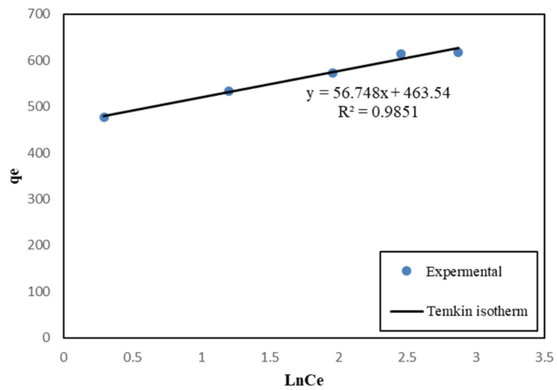

Figure 12. Plot of Temkin isotherm for adsorption of CR18 onto nano-clay.

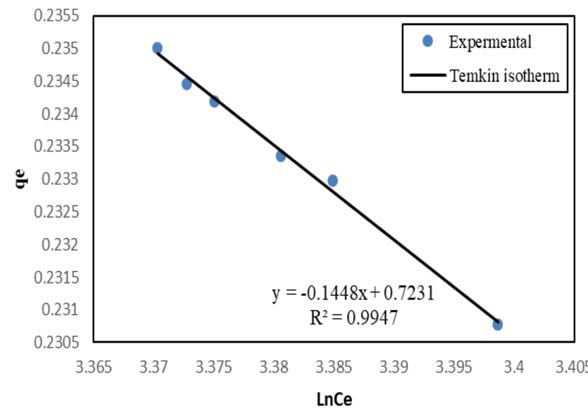

Figure 13. Plot of Temkin isotherm for adsorption of CR18 onto tonsil.

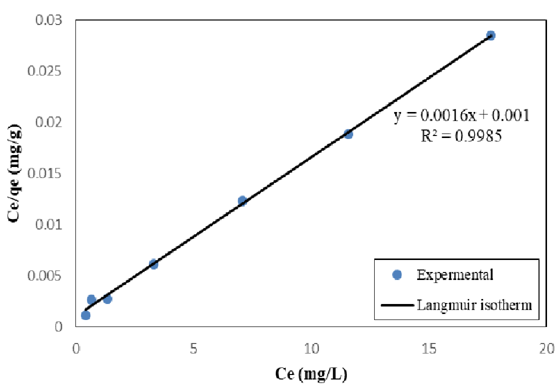

Figure 14. Plot of Langmuir isotherm for adsorption of CR18 onto nano-clay.

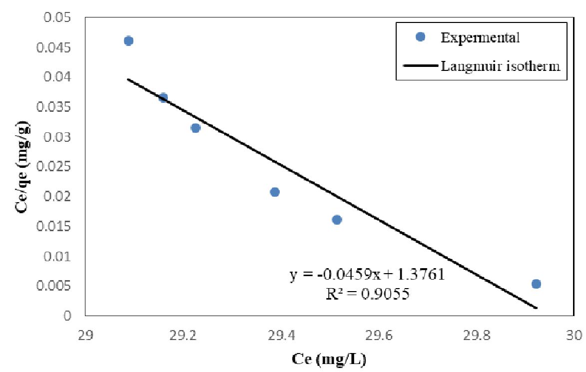

Figure 15. Plot of Langmuir isotherm for adsorption of CR18 onto tonsil.

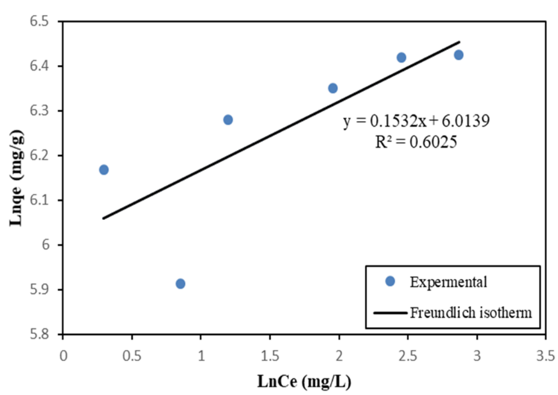

Figure 16. Plot of Freundlich isotherm for adsorption of CR18 onto nano-clay.

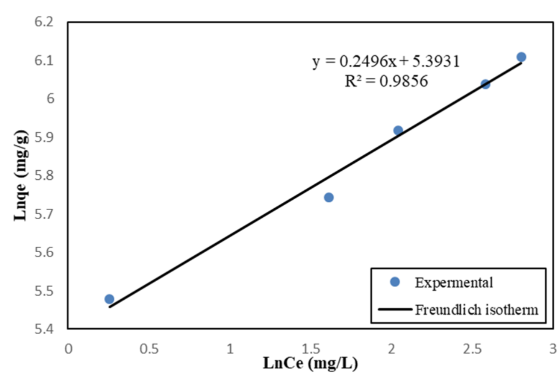

Figure 17. Plot of Freundlich isotherm for adsorption of CR18 onto Tonsil.

Based on the plots of the isotherms for nano-clay, it was found that the adsorption of CR18 strongly fited to the Langmuir isotherm (Figure 14). The finding emphasizes on a monolayer adsorption of CR18 onto a homogenous nano-clay surface. The results of the tonsil adsorption isotherms demonstrate that it is expressed very well by the Freundlich isotherm model (Figure 17), showing that the adsorption of CR18 takes place on the heterogeneous surface of tonsil with a non-uniform distribution of heat over the surface.

Table 2. Parameters of the Freundlich, Langmuir and Temkin isotherms, obtained for adsorption of CR18.

Langmuir isotherm			
Adsorbent	K_L	Q_0	R^2
Tonsil	0.0327	22.22	0.905
Nano-clay	1	1000	9.998
Freundlich isotherm			
Adsorbent	K_F	n	R^2
Tonsil	221.406	4.115	0.985
Nano-clay	437.029	7.407	0.955
Temkin isotherm			
Adsorbent	A	b	R^2
Tonsil	0.5085	17205.36	0.82
Nano-clay	0.319	28.448	0.994

3.7. Adsorption kinetics

The kinetic examinations of the adsorption of CR18 from the solution media onto the tonsil and nano-clay surfaces were conducted. Two common kinetic models including the pseudo-first- and second-order were taken into account in the current research work. The results obtained are demonstrated in Figures 18-21.

The pseudo-first-order kinetics is commonly denoted as follows [78].

$$dq_t/dt = k_1(q_e - q_t) \tag{5}$$

Here, k_1 is the equilibrium rate constant of the pseudo-first-order kinetics (1/min), q_e is the quantity of the dye adsorbed at the equilibrium (mmol/g), and q_t is the quantity of CR18 adsorbed at time t (mmol/g). After integrating and using the conditions $q_t = 0$ at $t = 0$ and, $q_t = q_t$ at $t = t$, we obtained [80]:

$$Ln\ (q_e - q_t) = Ln\ q_e - \left(\frac{k_1 t}{2.303}\right) \tag{6}$$

The pseudo-second-order chemisorption kinetic rate was obtained as follows [80]:

$$d(q_t t)/dt = k(q_e - q_t) \tag{7}$$

Here, k is the equilibrium rate constant of the pseudo-second order kinetics (g/mmol min) and q_e is the quantity of the dye adsorbed at the equilibrium state (mmol/g) [81]. On integrating Eq. (7), we obtained [80]:

$$t/q_t = 1/kq_e^2 + t/q_e \tag{8}$$

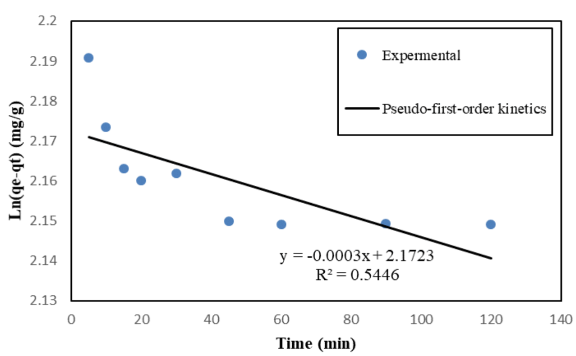

Figure 18. Pseudo-first-order adsorption kinetics of CR18 onto tonsil.

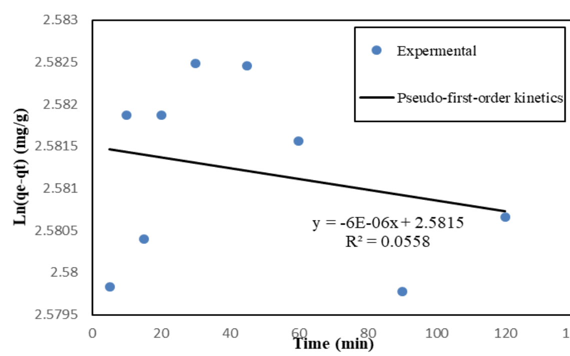

Figure 19. Pseudo-first-order adsorption kinetics of CR18 onto nano-clay.

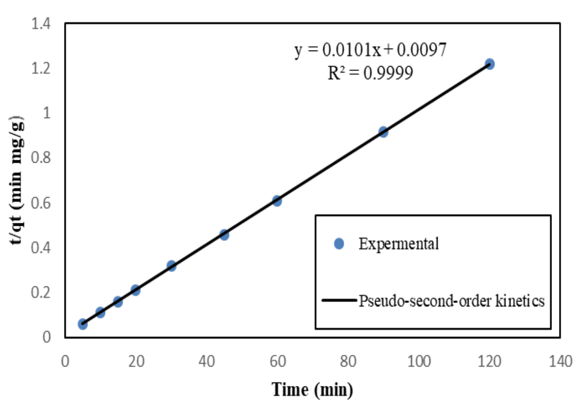

Figure 20. Pseudo-second-order adsorption kinetics of CR18 onto tonsil.

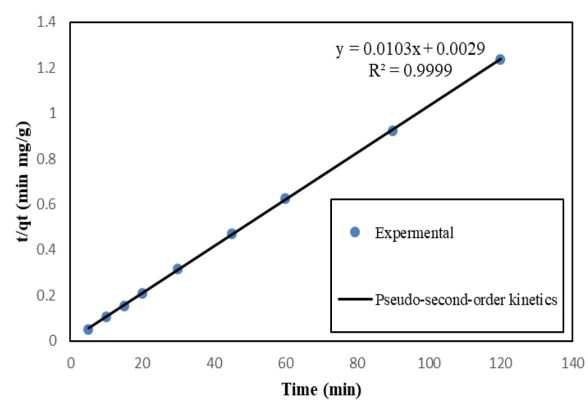

Figure 21. Pseudo-second-order adsorption kinetics of CR18 onto nano-clay.

The results of the adsorption kinetics display that the pseudo-second-order model explains the adsorption kinetics of tonsil and nano-clay most effectively. The high values of the correlation coefficients calculated for both adsorbents (> 0.999) in Figures 21 and 22, strongly approve that the experimental data obtained from the adsorption process could be well-predicted by the pseudo-second-order kinetics. This indicates that the adsorption mechanism is chemisorption, and that the rate of CR18 diffusion in the pores of tonsil and nano-clay limite the total rate of adsorption. Table 3 summarizes the kinetic parameters for the adsorption of CR18 by tonsil and nano-clay.

Table 3. Pseudo-first- and second-order kinetic parameters for adsorption of CR18 onto tonsil and nano-clay.

Adsorbent	Pseudo-first-order			Pseudo-second-order		
	R_1^2	$K_1(1/min)$	$q_e(mmol/g)$	R_2^2	$K_2(g/mg.min)$	$q_e(mmol/g)$
Tonsil	0.54	0	148.6	0.99	0.011	100
Nano-clay	0.83	0.0000184	481.066	0.99	0.005	100

3.8. Adsorption thermodynamics

The amounts of dye uptake at 288, 298, 308, 318, and 327K were studied in order to measure the thermodynamic factors by the Van't Hoff equation [82]:

$$Ln\ K_{ad} = \frac{\Delta S}{R} - \frac{\Delta H}{RT} \quad (9)$$

Here, K_{d} is the equilibrium constant, ΔS and ΔH are the entropy (kJ/mol K) and enthalpy (kJ/mol) variations of adsorption, respectively, R is the universal gas constant (8.314 J/mol K), and T is the absolute temperature (K). The values for ΔS and ΔH were computed from the slope and intercept of the linear regression of Ln K_{d} vs. (1/T), respectively. ΔG was estimated using the following equation [83]:

$$\Delta G = \Delta H - T\Delta S \quad (10)$$

Table 4 shows the thermodynamic parameters in different adsorption temperatures for tonsil and nano-clay. The adsorption of CR18 onto tonsil and nano-clay show the negative Gibbs free energies of -3.48 and -7.37 KJ/mol, respectively, indicating that both adsorption processes are spontaneous. As it can be observed in Table 4, the value of ΔH is negative for tonsil (-29.14 KJ/mol); however, it is a positive value for nano-clay (20.90KJ/mol). This indicates that the tonsil adsorption is exothermic, while the nano-clay adsorption process is an endothermic process.

Table 4. Thermodynamic parameters for adsorption of CR18 onto tonsil and nano-clay.

	$T\ (^0K)$	K_{ad}	$\Delta G\ (KJ/mol)$	$\Delta S\ (KJ/mol\ K)$	$\Delta H\ (KJ/mol)$
Tonsil	288	14.20	-3.48	-0.086	-29.14
	298	21.72			
	308	23.27			
	318	34.71			
	328	42.48			
Nano-clay	288	5.67	-7.37	0.095	20.90
	298	4.61			
	308	3.00			
	318	1.60			
	328	1.51			

3.9. Adsorbent mixture

Different ratios of the adsorbent mixtures were examined at their optimum conditions. Figure 22 displays the adsorption results of three different concentration ratios of tonsil:nano-clay with adsorption times.

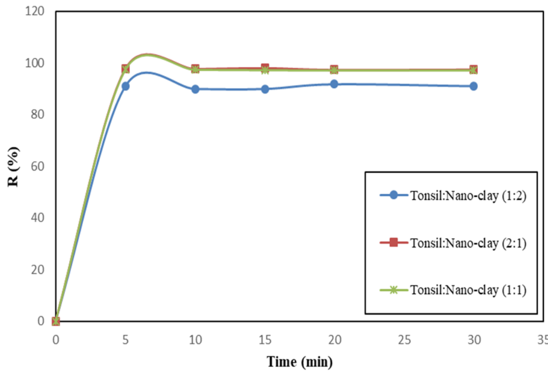

Figure 22. Effect of tonsil: nano-clay concentration ratios on the adsorption efficiency under optimum conditions of tonsil.

The results obtained reveal the fact that the maximum adsorption of CR18 could be achieved by increasing the tonsil: nano-clay concentration ratio.

4. Conclusions

In this research work, the possibility of CR18 adsorption onto tonsil and nano-clay was studied. The effects of some important factors comprising the amount of adsorbent, pH, contact time, original concentration of CR18, and stirring speed were studied. It was detected that the nano-clay adsorption mechanism well-followed the Langmuir isotherm, while tonsil fitted better to the Freundlich isotherm. Kinetic studies displayed that the pseudo-second-order model could effectively explain the behavior of adsorption of CR18 onto both the nano-clay and tonsil surfaces. The results of the thermodynamic experiments indicated that the tonsil and nano-clay adsorptions were exothermic and endothermic, respectively, and that both were spontaneous. Studies on the adsorbent mixtures demonstrated that increasing tonsil to the nano-clay concentration ratio improved the adsorption efficiency in the system. Under the optimum conditions including the pH of 7, stirring speed of 200 rpm, CR18 concentration of 30 ppm, contact time of 30 min, and tonsil:nano-clay ratio of 1:2 (0.06g:0.015g), the maximum adsorption efficiency was achieved. The clay mineral can provide a replacement for the costly adsorption materials such as active carbon due to its accessibility and comparatively low cost. According to many studies, activated carbon is a useful adsorbent for organic contaminants; though, its high initial cost and the requirement for an expensive regeneration system make it less economically feasible as an adsorbent. Cost effectiveness, accessibility, and adsorptive properties are the principal criteria for selecting an adsorbent in order to remove the organic and inorganic contaminants. Taking these criteria into attention, it can be said that the naturally existing clay can be utilized as a more low-cost adsorbent for the adsorption of dyes without requiring a costly regeneration instead of expensive adsorption materials.

Acknowledgements

The authors express their sincere thanks to Dr. Mohammad Ebrahim Olya as the faculty member of Institute for Color Science & Technology for their constant support and helps about the experimental studies.

Conflict of interest

The authors claim that they have no conflict of interest.

References

[1]. Crini G (2006) Non-conventional low-cost adsorbents for dye removal: a review. Bioresource technology 97(9): 1061-1085.

[2]. Molen J (2008) Treatability studies on the wastewater from a dye manufacturing industry. Unpublished master's thesis. Asian Institute of Technology, Thailand.

[3]. Ding S, Li Z, and Wang R (2010) Summary of treatment of dyestuff wastewater. Water Resources Protection 26(3): 73-78.

[4]. Chen K-C, Wu J-Y, Huang C-C, Liang Y-M, and Hwang S-CJ (2003) Decolorization of azo dye using PVA-immobilized microorganisms. Journal of Biotechnology 101(3): 241-252.

[5]. Puvaneswari N, Muthukrishnan J, and Gunasekaran P (2006) Toxicity assessment and microbial degradation of azo dyes. Indian journal of experimental biology 44(8): 618-626.

[6]. Omar HH (2008) Algal decolorization and degradation of monoazo and diazo dyes. Pak J Biol Sci 11(10): 1310-1316.

[7]. Smith P , and Coackley P (1983) A method for determining specific surface area of activated sludge by dye adsorption. Water Research 17(5): 595-598.

[8]. Jia J, Yang J, Liao J, Wang W, and Wang Z (1999) Treatment of dyeing wastewater with ACF electrodes. Water research 33(3): 881-884.

[9]. Al-Degs Y, Khraisheh M, Allen S, and Ahmad M (2000) Effect of carbon surface chemistry on the removal of reactive dyes from textile effluent. Water Research 34(3): 927-935.

[10]. Sivaraj R, Namasivayam C, and Kadirvelu K (2001) Orange peel as an adsorbent in the removal of acid violet 17 (acid dye) from aqueous solutions. Waste management 21(1): 105-110.

[11]. Gupta V (2009) Application of low-cost adsorbents for dye removal–A review. Journal of environmental management 90(8): 2313-2342.

[12]. Ula MM , Latif WA (2012) Fixed bed adsorption for wastewater treatment. Universiti Malaysia Pahang.

[13]. Morais L, Freitas O, Goncalves E, Vasconcelos L, and Beca CG (1999) Reactive dyes removal from wastewaters by adsorption on eucalyptus bark: variables that define the process. Water Research 33(4): 979-988.

[14]. Sivakumar S, Senthilkumar P, and Subburam V (2001) Carbon from cassava peel, an agricultural waste, as an adsorbent in the removal of dyes and metal ions from aqueous solution. Bioresource Technology 80(3): 233-235.

[15]. Annadurai G, Juang R-S, and Lee D-J (2002) Use of cellulose-based wastes for adsorption of dyes from aqueous solutions. Journal of hazardous materials 92(3): 263-274.

[16]. Ramesha G, Kumara AV, Muralidhara H, and Sampath S (2011) Graphene and graphene oxide as effective adsorbents toward anionic and cationic dyes. Journal of colloid and interface science 361(1): 270-277.

[17]. Salleh MAM, Mahmoud DK, Karim WA, and Idris A (2011) Cationic and anionic dye adsorption by agricultural solid wastes: A comprehensive review. Desalination 280(1): 1-13.

[18]. Bajpai A, and Rajpoot M (1999) Adsorption techniques: a review. J Sci Ind Res 58(11): 844-860.

[19]. Manev ED, and Nguyen AV (2005) Effects of surfactant adsorption and surface forces on thinning and rupture of foam liquid films. International Journal of Mineral Processing 77(1): 1-45.

[20]. Lima E, Horinek D, Netz R, Biscaia E, Tavares F, Kunz W, and Boström (2008) Specific ion adsorption and surface forces in colloid science. The Journal of Physical Chemistry B 112(6): 1580-1585.

[21]. Parker HL, Hunt AJ, Budarin VL, Shuttleworth PS, Miller KL, and Clark JH (2012) The importance of being porous: polysaccharide-derived mesoporous materials for use in dye adsorption. RSC Advances 2(24): 8992-8997.

[22]. Gharabaghi M, and Aghazadeh S (2014) A review of the role of wetting and spreading phenomena on the flotation practice. Current Opinion in Colloid & Interface Science 19(4): 266-282.

[23]. Aghazadeh S, Mousavinezhad SK, and Gharabaghi M (2015) Chemical and colloidal aspects of collectorless flotation behavior of sulfide and non-sulfide minerals. Advances in colloid and interface science 225: 203-217.

[24]. Atkin R, Craig V, Wanless EJ, and Biggs S (2003) Mechanism of cationic surfactant adsorption at the solid–aqueous interface. Advances in colloid and interface science 103(3): 219-304.

[25]. Dąbrowski A (2001) Adsorption—from theory to practice. Advances in colloid and interface science 93(1): 135-224.

[26]. Foo K, and Hameed B (2010) Insights into the modeling of adsorption isotherm systems. Chemical Engineering Journal 156(1): 2-10.

[27]. Fu Y, and Viraraghavan T (2001) Fungal decolorization of dye wastewaters: a review. Bioresource technology 79(3): 251-262.

[28]. Annadurai G, Ling LY, and Lee J-F (2008) Adsorption of reactive dye from an aqueous solution by chitosan: isotherm, kinetic and thermodynamic analysis. Journal of hazardous materials 152(1): 337-346.

[29]. Ramakrishna KR, and Viraraghavan T (1997) Dye removal using low cost adsorbents. Water Science and Technology 36(2-3): 189-196.

[30]. Harris RG, Wells JD, and Johnson BB)2001(Selective adsorption of dyes and other organic molecules to kaolinite and oxide surfaces. Colloids and Surfaces A: Physicochemical and Engineering Aspects 180(1): 131-140.

[31]. Ghosh D, and Bhattacharyya KG (2002) Adsorption of methylene blue on kaolinite. Applied Clay Science 20(6): 295-300.

[32]. Özcan AS , and Özcan A (2004) Adsorption of acid dyes from aqueous solutions onto acid-activated bentonite. Journal of Colloid and Interface Science 276(1): 39-46.

[33]. Tahir S, and Rauf N (2006) Removal of a cationic dye from aqueous solutions by adsorption onto bentonite clay. Chemosphere 63(11): 1842-1848.

[34]. Yue Q-Y, Li Q, Gao B-Y, Yuan A-J, and Wang Y (2007) Formation and characteristics of cationic-polymer/bentonite complexes as adsorbents for dyes. Applied Clay Science 35(3): 268-275.

[35]. Bulut E, Özacar M, and Şengil İA (2008) Equilibrium and kinetic data and process design for adsorption of Congo Red onto bentonite. Journal of Hazardous Materials 154(1): 613-622.

[36]. Lian L, Guo L, and Guo C (2009) Adsorption of Congo red from aqueous solutions onto Ca-bentonite. Journal of Hazardous Materials 161(1): 126-131.

[37]. Shen D, Fan J, Zhou W, Gao B, Yue Q, and Kang Q (2009) Adsorption kinetics and isotherm of anionic dyes onto organo-bentonite from single and multisolute systems. Journal of hazardous materials 172(1): 99-107.

[38]. Meshko V, Markovska L, Mincheva M, and Rodrigues A (2001) Adsorption of basic dyes on

granular acivated carbon and natural zeolite. Water research 35(14): 3357-3366.

[39]. Alpat SK, Özbayrak Ö, Alpat Ş, and Akçay H (2008) The adsorption kinetics and removal of cationic dye, Toluidine Blue O, from aqueous solution with Turkish zeolite. Journal of hazardous materials 151(1): 213-220.

[40]. Han R, Zhang J, Han P, Wang Y, Zhao Z, and Tang M (2009) Study of equilibrium, kinetic and thermodynamic parameters about methylene blue adsorption onto natural zeolite. Chemical Engineering Journal 145(3): 496-504.

[41]. Özacar M, and Şengil İA (2002) Adsorption of acid dyes from aqueous solutions by calcined alunite and granular activated carbon. Adsorption 8(4): 301-308.

[42]. Özacar M, and Şengil IA (2003) Adsorption of reactive dyes on calcined alunite from aqueous solutions. Journal of hazardous materials 98(1): 211-224.

[43]. Doğan M, and Alkan M (2003) Removal of methyl violet from aqueous solution by perlite. Journal of colloid and interface science 267(1): 32-41.

[44]. Özacar M, and Şengil İA (2004) Application of kinetic models to the sorption of disperse dyes onto alunite. Colloids and Surfaces A: Physicochemical and Engineering Aspects 242(1): 105-113.

[45]. Champagne P-P, and Ramsay J (2007) Reactive blue 19 decolouration by laccase immobilized on silica beads. Applied microbiology and biotechnology 77(4): 819-823.

[46]. Roulia M , and Vassiliadis AA (2008) Sorption characterization of a cationic dye retained by clays and perlite. Microporous and Mesoporous Materials 116(1): 732-740.

[47]. Vijayakumar G, Dharmendirakumar M, Renganathan S, Sivanesan S, Baskar G, and Elango KP (2009) Removal of Congo red from aqueous solutions by perlite. CLEAN–Soil, Air, Water 37(4-5): 355-364.

[48]. Namasivayam C, and Kavitha D (2002) Removal of Congo Red from water by adsorption onto activated carbon prepared from coir pith, an agricultural solid waste. Dyes and pigments 54(1): 47-58.

[49]. Malik K (2003) Use of activated carbons prepared from sawdust and rice-husk for adsorption of acid dyes: a case study of Acid Yellow 36. Dyes and pigments 56(3): 239-249.

[50]. Adekola F, and Adegoke H (2005) Adsorption of blue-dye on activated carbons produced from rice husk, coconut shell and coconut coir pith. Ife Journal of Science 7(1): 151-157.

[51]. Han R, Ding D, Xu Y, Zou W, Wang Y, Li Y, and Zou L (2008) Use of rice husk for the adsorption of congo red from aqueous solution in column mode. Bioresource Technology 99(8): 2938-2946.

[52]. Gong J-L, Wang B, Zeng G-M, Yang C-P, Niu C-G, Niu Q-Y, Zhou W-J, and Liang Y (2009) Removal of cationic dyes from aqueous solution using magnetic multi-wall carbon Nanotube Nanocomposite as adsorbent. Journal of Hazardous Materials 164(2): 1517-1522.

[53]. Verma V, Mishra A (2010) Kinetic and isotherm modeling of adsorption of dyes onto rice husk carbon. Global NEST Journal 12(2): 190-196.

[54]. Safa Y, and Bhatti HN (2011) Kinetic and thermodynamic modeling for the removal of Direct Red-31 and Direct Orange-26 dyes from aqueous solutions by rice husk. Desalination 272(1): 313-322.

[55]. Chowdhury S, Mishra R, Saha P, and Kushwaha P (2011) Adsorption thermodynamics, kinetics and isosteric heat of adsorption of malachite green onto chemically modified rice husk. Desalination 265(1): 159-168.

[56]. Tan KA, Morad N, Teng TT, Norli I, and Panneerselvam P (2012) Removal of cationic dye by magnetic Nanoparticle (Fe3O4) impregnated onto activated maize cob powder and kinetic study of dye waste adsorption. APCBEE Procedia 1: 83-89.

[57]. Aljeboree AM, Alshirifi AN, and Alkaim AF (2014) Kinetics and equilibrium study for the adsorption of textile dyes on coconut shell activated carbon. Arabian Journal of Chemistry 10: S3381-S3393.

[58]. Netpradit , Thiravetyan P, and Towprayoon S (2004) Adsorption of three azo reactive dyes by metal hydroxide sludge: effect of temperature, pH, and electrolytes. Journal of colloid and interface science 270(2): 255-261.

[59]. Gupta VK, Ali I, and Saini VK (2007) Adsorption studies on the removal of Vertigo Blue 49 and Orange DNA13 from aqueous solutions using carbon slurry developed from a waste material. Journal of Colloid and Interface Science 315(1): 87-93.

[60]. Santos SC, Vilar VJ, and Boaventura RA (2008) Waste metal hydroxide sludge as adsorbent for a reactive dye. Journal of Hazardous Materials 153(3): 999-1008.

[61]. Wong Y, Szeto Y, Cheung W, and McKay G (2003) Equilibrium studies for acid dye adsorption onto chitosan. Langmuir 19(19): 7888-7894.

[62]. Wong Y, Szeto Y, Cheung W, and McKay G (2004) Adsorption of acid dyes on chitosan—equilibrium isotherm analyses. Process Biochemistry 39(6): 695-704.

[63]. Allen S, Mckay G, and Porter J (2004) Adsorption isotherm models for basic dye adsorption by peat in single and binary component systems. Journal of colloid and interface science 280(2): 322-333.

[64]. Hu Z, Zhang J, Chan W, and Szeto Y (2006) The sorption of acid dye onto chitosan Nanoparticles. Polymer 47(16): 5838-5842.

[65]. Cheung W, Szeto Y, and McKay G (2007) Intraparticle diffusion processes during acid dye adsorption onto chitosan. Bioresource Technology 98(15): 2897-2904.

[66]. Han X, Wang W, and Ma X (2011) Adsorption characteristics of methylene blue onto low cost biomass material lotus leaf. Chemical Engineering Journal 171(1): 1-8.

[67]. Cheng R, Xiang B, Li Y, and Zhang M (2011) Application of dithiocarbamate-modified starch for dyes removal from aqueous solutions. Journal of hazardous materials 188(1): 254-260.

[68]. Abdel-Halim E (2013) Preparation of starch/poly (N, N-Diethylaminoethyl methacrylate) hydrogel and its use in dye removal from aqueous solutions. Reactive and Functional Polymers 73(11): 1531-1536.

[69]. Crini G (2003) Studies on adsorption of dyes on beta-cyclodextrin polymer. Bioresource technology 90(2): 193-198.

[70]. Crini G (2008) Kinetic and equilibrium studies on the removal of cationic dyes from aqueous solution by adsorption onto a cyclodextrin polymer. Dyes and Pigments 77(2): 415-426.

[71]. Cheng R, Ou S, Xiang B, Li Y, and Liao Q (2009) Equilibrium and molecular mechanism of anionic dyes adsorption onto copper (II) complex of dithiocarbamate-modified starch. Langmuir 26(2): 752-758.

[72]. Tunc Ö, Tanacı H, and Aksu Z (2009) Potential use of cotton plant wastes for the removal of Remazol Black B reactive dye. Journal of Hazardous Materials 163(1): 187-198.

[73]. Wang Q, Luan Z, Wei N, Li J, and Liu C (2009) The color removal of dye wastewater by magnesium chloride/red mud (MRM) from aqueous solution. Journal of hazardous materials 170(2): 690-698.

[74]. Mahmoodi NM, Arami M, Limaee NY, Gharanjig K, and Nourmohammadian F (2007) Nanophotocatalysis using immobilized titanium dioxide Nanoparticle: degradation and mineralization of water containing organic pollutant: case study of Butachlor. Materials Research Bulletin 42(5): 797-806.

[75]. Banihashemi A, Moghadam MRA, Maknoon R, and Nikazar M (2008) Development of a coagulation/flocculation predictive model for turbidity removal from Tehran water treatment plants. Environmental Engineering & Management Journal (EEMJ) 7(1): 13-16.

[76]. Langmuir I (1916) The constitution and fundamental properties of solids and liquids. Part I. Solids. Journal of the American Chemical Society 38(11): 2221-2295.

[77]. Uber F (1985) Die adsorption in losungen. Z. Phys. Chem 57: 387-470.

[78]. Cheremisinoff NP (2001) Handbook of water and wastewater treatment technologies. Butterworth-Heinemann.

[79]. Fathizadeh M, and Nikazar M (2009) Adsorption of aromatic from alkane/aromatic mixtures by NaY zeolite. Journal of chemical engineering of Japan 42(4): 241-247.

[80]. Ho YS, and McKay G (1999) Pseudo-second order model for sorption processes. Process Biochem 34: 451-465.

[81]. Mahmoodi NM, and Najafi F (2012) Preparation of surface modified zinc oxide nanoparticle with high capacity dye removal ability. Materresbull. 47: 1800–1809.

[82]. Jaycock MJ, and Parfitt GD (1981) Chemistry of interfaces. Onichester, Ellis Horwood Ltd.

[83]. Lui P (2007) Polymer modified clay minerals, A review. Appl Clay Sci 38: 64-76.

مطالعه اثر اصلاح جاذب‌های نانو معدنی بر راندمان حذف رنگ از پساب‌های صنعتی

آزاده آگاه[۱]* و نسرین فلاحتی[۲]

۱- گروه مهندسی معدن، دانشگاه سیستان و بلوچستان، زاهدان، ایران

۲- بخش مهندسی معدن، دانشگاه صنعتی اراک، اراک، ایران

ارسال ۲۰۲۰/۰۹/۳۰، پذیرش ۲۰۲۰/۱۲/۰۶

* نویسنده مسئول مکاتبات: agah_eng@eng.usb.ac.ir

چکیده:

در این کار تحقیقاتی، اثر بالقوه نانورس و تونسیل به عنوان جاذب‌های ارزان قیمت وداخلی در حذف رنگزای کاتیونی قرمز ۱۸ ازآب آلوده در سیستم‌های ناپیوسته مطالعه شده است. خصوصیات سطحی جاذب ها با استفاده از میکروسکوپ الکترونی پویشی (SEM) و پراش پرتو ایکس (XRD) مورد مطالعه قرار گرفت. تاثیر عوامل مختلف موثر بر فرآیند جذب رنگ بررسی شد. در کار حاضر اثر زمان تماس، میزان جاذب، غلظت اولیه، pH و دور همزن مورد بررسی قرار گرفته است. نتایج نشان داد میزان حذف رنگ در مقادیر بهینه این پارامترها به بیش از ۹۵ درصد رسیده است. در پایان میزان مطابقت داده‌های به دست آمده در این پژوهش با ایزوترمهای فرندلیچ، لانگموير و تمکین بررسی شد. فرآیند جذب رنگ جاذب نانو رس از ایزوترم لانگموير و برای تونسیل از ایزوترم فرندلیچ تبعیت می‌کند. سینتیک جذب توسط دو مدل سینتیکی شبه مرنبه اول و دوم مورد مطالعه قرار گرفت. مدل شبه مرتبه دوم بهترین انتخاب بین دو مدل سینتیکی برای شرح رفتار جذب مواد رنگزا در این سیستم بود. عوامل ترمودینامیکی در ارتباط با فرآیند جذب محاسبه شد. مقادیر منفی ΔG نشان می‌دهد که فرآیند جذب خود به خودی و ساز و کار جذب از نوع فیزیکی است. بنابراین این جاذب‌های طبیعی می‌توانند درحد وسیعی به عنوان جاذب‌های با صرفه اقتصادی و کارایی بالا مورد استفاده قرارگیرند. سرانجام پس از مشاهده نتایج آزمایش هر یک از جاذب‌ها به بررسی کارایی ترکیب دو جاذب در شرایط بهینه هر جاذب با نسبت‌های مختلف پرداخته شد. نتایج نشانگر این بود که ظرفیت جذب مخلوط دوتایی جاذب‌ها در شرایط بهینه نانو رس(pH =۷، 30 ppm=غلظت، ۲۰۰ rpm= دور جارتست) با نسبت ۲-۱ نانو کلی به تونسیل(۰/۰۱۵ نانوکلی و ۰/۰۶ تونسیل) بیشترین ظرفیت جذب را دارد.

کلمات کلیدی: جذب، تونسیل، نانو رس، حذف رنگ، پساب‌های صنعتی.